HHS Public Access

Author manuscript

SLAS Discov. Author manuscript; available in PMC 2021 September 01.

Published in final edited form as:

SLAS Discov. 2020 September ; 25(8): 939–949. doi:10.1177/2472555220915821.

Development and optimization of a high content analysis platform to identify suppressors of lamin B1 overexpression as a therapeutic strategy for Autosomal Dominant Leukodystrophy

Bruce Nmezi[1,*], **Laura L. Vollmer**[2,*], **Tong Ying Shun**[2], **Albert Gough**[2,3], **Harshvardhan Rolyan**[1,4], **Fang Liu**[1], **Yumeng Jia**[1], **Quasar S. Padiath**[1,†], **Andreas Vogt**[2,3,†]

[1]Department of Human Genetics, Graduate School of Public Health, University of Pittsburgh, Pittsburgh PA 15261

[2]Drug Discovery Institute, University of Pittsburgh Medical School, Pittsburgh PA 15260

[3]Department of Computational and Systems Biology, University of Pittsburgh Medical School, Pittsburgh PA 15260

[4]Current address: Department of Internal Medicine, Yale University, New Haven, CT

Abstract

Autosomal Dominant Leukodystrophy (ADLD) is a fatal, progressive adult-onset disease characterized by widespread central nervous system (CNS) demyelination and significant morbidity. The late age of onset together with the relatively slow disease progression provides a large therapeutic window for the disorder. However, no treatment exists for ADLD, representing an urgent and unmet clinical need. We have previously shown that ADLD is caused by duplications of the lamin B1 gene causing increased expression of the lamin B1 protein, a major constituent of the nuclear lamina, and demonstrated that transgenic mice with oligodendrocyte specific over-expression of lamin B1 exhibit temporal and histopathological features reminiscent of the human disease. As increased levels of lamin B1 are the causative event triggering ADLD, approaches aimed at reducing lamin B1 levels and associated functional consequences represent a promising strategy for discovery of small molecule ADLD therapeutics. To this end, we have created an inducible cell culture model of lamin B1 overexpression and developed high-content analysis in connection with multivariate analysis to define, analyze, and quantify lamin B1 expression and its associated abnormal nuclear phenotype in mouse fibroblasts (MEF). The assay has been optimized to meet high throughput screening (HTS) criteria in multi-day variability studies. To control for batch-to-batch variation in the primary MEFs we have implemented a screening strategy that employs sentinel cells to avoid costly losses during HTS. We posit the assay will identify bona fide suppressors of lamin B1 pathophysiology as candidates for development into potential therapies for ADLD.

[†]Address correspondence to: Andreas Vogt, Department of Computational and Systems Biology and University of Pittsburgh Drug Discovery Institute, W948 Biomedical Science Tower, University of Pittsburgh, Pittsburgh, PA 15260; Telephone: (412)-383-5856; Fax: (412)-648-9009; avogt@pitt.edu; Quasar S Padiath, Department of Human Genetics, 3135 Pitt Public Health, University of Pittsburgh, Pittsburgh, PA 15261; Telephone: (412)-624-7203; Fax: (412)-624-3020; qpadiath@pitt.edu.

[*]These authors contributed equally to the work

Keywords

High throughput screening; high-content analysis; multivariate analysis; lamin B1; autosomal dominant leukodystrophy

INTRODUCTION

Autosomal Dominant Leukodystrophy (ADLD) is an ultra-rare fatal, progressive adult onset disease. It occurs in the 4th or 5th decade of life and the primary pathology is widespread CNS demyelination[1]. Symptoms usually begin with signs of autonomic dysfunction followed by loss of fine motor control. This is followed by spasticity, ataxia, tremor and paralysis of upper and lower extremities. ADLD is thus associated with significant morbidity before patients ultimately succumb to the disease, usually within 10–20 years after the onset[2]. Robust genetic testing, the late age at onset and the relative slow progression of the disease provide a large window for therapeutic intervention and thus make ADLD an ideal candidate for the identification of potential drugs. However, no cure or treatment exists for the disease, representing an urgent and unmet clinical need.

ADLD is caused by heterozygous duplications of the lamin B1 gene and genomic deletions upstream of lamin B1, both resulting in increased LMNB1 protein expression [3–6]. Lamin B1 is an intermediate filament protein that is an integral part of the nuclear lamina, a fibrous meshwork found adjacent to the inner nuclear membrane in all cells. In vertebrates, there are of two main types of lamins: The A and B type. The A type lamins, lamins A & C, are alternatively spliced products of the same gene *LMNA.* Two separate genes, *LMNB1* and *LMNB2*, code for the major B type lamins[7–10]. While originally identified as having a structural role in maintaining nuclear architecture, the nuclear lamina is now thought to play critical roles in multiple cellular processes including transcription, DNA replication, DNA repair and epigenetic regulation [7, 10, 11]. Nuclear abnormalities have been reported in ADLD patient fibroblasts, fibroblasts from ataxia telangiectasia patients exhibiting increased lamin B1 levels, and in HEK293 cells transfected with lamin B1 constructs[3, 12, 13]. Mouse models overexpressing lamin B1 in oligodendrocytes, the cell types that produce myelin in the CNS, recapitulate the late age at onset and many of the histopathological features of ADLD, further strengthening the link between lamin B1 overexpression and the demyelination phenotype [14, 15]. As an increased level of lamin B1 is the causative agent triggering ADLD, we reasoned that approaches aimed at reducing lamin B1 levels, rather than downstream targets, whose roles in ADLD are currently poorly understood, would represent a potent and innovative strategy that could be exploited for therapeutic discovery. This study describes the development of a high content analysis platform to identify suppressors of lamin B1 overexpression that may serve as potential therapeutic molecules for the treatment of ADLD.

MATERIALS AND METHODS

Generation of TRE-LMNB1 cell lines.

TRE-FLAG-LMNB1 hemizygous mice, described previously[14], were independently generated at the University of Pittsburgh transgenic core on an FVB/N background and were

mated with *Rosa26-rtTA* homozygous mice (Jackson Laboratories) to produce *TRE-FLAG-LMNB1;Rosa rtTA* and wild-type offspring (Figure 1A). Primary mouse embryonic fibroblasts (MEFs) were isolated from 13.5 day old embryos as previously described[16]. All animals were housed at University of Pittsburgh animal facilities in accordance with IACUC guidelines.

Cell culture.

Primary MEFs from wild-type and *TRE-FLAG-LMNB1;Rosa-rtTA* embryos were cultured in complete DMEM (high glucose DMEM (Corning) supplemented with 10% FBS (Fisher), 2mM L-glutamine (Millipore), and 1% Penicillin streptomycin (Hyclone) in a humidified chamber at 37°C and 5% CO2. When cells reached 90–100% confluence, they were trypsinized, diluted, and re-plated using fresh media. Lamin B1 overexpression was induced in *TRE-FLAG-LMNB1;Rosa-rtTA* transgenic MEFs by adding 2 μg/mL doxycycline in growth medium. Primary human skin fibroblasts from an ADLD patient were isolated as previously described[6], and cultured in complete DMEM in a humidified chamber at 37°C and 5% CO_2.

Preliminary imaging and quantification.

Cells seeded on glass coverslips were washed with DPBS (Sigma), then fixed with 4% formaldehyde (Ted Pella), and simultaneously blocked and permeabilized in PBS + 5% normal donkey serum (Jackson ImmunoResearch) + 0.3% Triton X-100 (Sigma) for 1 hour at room temperature. Cells were probed overnight at 4°C with primary antibodies anti-lamin B1 and anti-lamin A/C diluted 1:500 each in PBS + 1% BSA (Sigma) + 0.3% Triton X-100. The next morning, cells were washed in PBS at room temperature then probed with anti-rabbit and anti-mouse secondary antibodies each diluted 1:350 in PBS + 1% BSA for 1 hour at room temperature in the dark, washed again in PBS, then mounted onto glass microscope slides using Vectashield antifade mounting medium with DAPI (Vector Laboratories). Wide-field microscopy images were acquired of immunofluorescently-labeled nuclei on a Leica DM5000B upright microscope with a 40× 0.75 NA objective, a 63× 1.40 NA oil immersion objective, and a Leica DFC310 FX digital camera. Preliminary quantification of abnormal nuclei was performed manually by counting nuclei with excessive surface folding, contortions, convolutions, or invaginations of the nuclear envelope. For each experiment, cells from 9–17 imaging fields were counted and assigned as “normal” and “abnormal” by a human observer. Fractions of abnormal nuclei in each field were averaged and analyzed for significance using the modified Wald method [17] in GraphPad Prism.

Reagents.—Antibodies used were: Anti-Lamin B1 (Abcam AB16048); anti-lamin A/C (Cell Signaling Technology 4777); donkey-anti-rabbit-Cy3 (711-165-150); donkey-anti-mouse-Cy5 (715-175-150) for MEFs, and donkey-anti-rabbit-FITC (711-095-152, all from Jackson Immunoresearch) for ADLD patient cells. All other reagents including doxycycline (D-9891) and BSA (A-2153) were from Sigma-Aldrich (St. Louis, MO).

High content analysis.

TRE-MEF were plated in collagen-coated 384 well microplates (Greiner 781956), fixed with formaldehyde (4%), permeabilized with Triton X-100 (0.3%)/BSA (1%) in PBS, and stained

with anti-lamin B1 and anti-lamin A/C antibodies overnight at 4°C, followed by Cy3- and Cy-5 conjugated secondary antibodies, respectively. Nuclei were counterstained with Hoechst 33342. Plates were washed with PBS, sealed, and images acquired on an Thermo Fisher Cellomics ArrayScan II high content reader using a 10X 0.75 NA objective. 1000 cells per well were acquired and analyzed for lamin expression and texture using the Target Activation Bioapplication. Nuclear shape measurements were made on Hoechst labeling. All measurements were made in an area defined by Hoechst staining. The Bioapplication generated twenty-four parameters (Supplemental Table 1). To quantify lamin B1 intensity distributions, three heterogeneity indices (Kolmogorov-Smirnov (KS_Norm), Quadratic Entropy (QE), and percent outliers) were calculated as described [18] based on lamin B1 staining.

Higher resolution images were acquired on a Molecular Devices ImageXpress Ultra confocal HCS reader with a 40X objective (to illustrate cell population heterogeneity) or as three-dimensional z-stacks (20 planes, 0.3 μm) using a 60X objective followed by 3D reconstruction in MetaXpress (to document the nuclear abnormalities phenotype).

Sentinel cell analysis.

From a single vial of MEFs, two 10% aliquots are set aside and treated with DOX or vehicle (0.001% ethanol) for three days. The remaining 80% of cells are plated into a single T-150 flask and expanded for large scale HTS. The small aliquots are trypsinized on day 3, plated into medium with or without DOX, and immunostained with anti-lamin B1 and anti-lamin A/C antibodies. HCA is performed to determine DOX responsiveness of the particular vial. Batches that do not meet HTS criteria in the sentinel cells are discarded; otherwise cells are used for experiments.

Multivariate analysis.

To enable measurements of nuclear abnormalities with sufficient statistical rigor for HTS we employed linear discriminant analysis (LDA), to integrate multiple readouts into the Z'-factor as previously described by us [19, 20] and others [21, 22]. The details of the method have been documented in detail [20] and are only briefly reiterated here. From the multidimensional high content data set, twenty-seven parameters and the three heterogeneity indices described above were reduced to a single statistical parameter (the LDA value) using the LDA function included in the MASS package of the R statistical software program (https://cran.r-project.org). Z' factors were then calculated as described [23] using LDA values from WT and TRE-LMNB1 MEF treated with DOX (2 μg/ml) as minimum (MIN) and maximum (MAX) controls, respectively.

RESULTS

Generation and characterization of an inducible cellular primary mouse fibroblast model of lamin B1 overexpression.

Fibroblasts from ADLD patient cells express higher levels of lamin B1 (Ref [6] and Supplemental Figure 1) but ADLD patient cells cannot be generated in numbers large enough for HTS, and donor-to-donor variability constitutes a problem. We therefore

established a tractable cell culture model for the study of nuclear alterations that would also be suited for high-throughput screening, and generated a mouse embryonic fibroblasts (MEF) system overexpressing lamin B1[14, 24]. We have generated inducible transgenic mice where the over-expression of a FLAG tagged human-lamin B1 gene is under the control of a tetracycline responsive element (TRE). These mice are then mated to a second mouse strain (ROSA rtTA, which contains the reverse tetracycline transactivator (rtTA) [25, 26]. MEFs derived from bi-transgenic embryos (i.e. Rosa rtTA:TRE-LMNB1, henceforth referred to as TRE-LMNB1) (Figure 1A) overexpress FLAG-tagged lamin B1 upon addition of doxycycline (DOX), a more stable derivative of tetracycline (Figure 1B). The levels of lamin B1 overexpression are ~ 2 fold at the protein level (Figure 1C), comparable to what has been observed in ADLD patient fibroblasts [6, 12]. The lamin B1 overexpressing MEFs also exhibit structural abnormalities similar to those that we and others have observed in ADLD patient fibroblasts [12, 13], and show significant increases in misshapen nuclei (Figure 1D). These alterations were reversible, as subsequent to the removal of DOX and the cessation of lamin B1 overexpression, nuclear structure returned to normal (Figure 1E). Our results are consistent with a previous report demonstrating that RNAi mediated knockdown of lamin B1 levels in ADLD patient fibroblasts and cells derived from ADLD patient induced pluripotent stem cells (iPSCs) restores nuclear rigidity and morphology to those indistinguishable from control cells [12]. Taken together, these results strongly suggest that normalizing lamin B1 levels can functionally rescue the lamin B1 overexpression phenotype. As the transgene in the MEFs is stably integrated into the genome of these cells, they have a uniform and persistent lamin B1 overexpression in the presence of DOX. Furthermore, we can generate MEFs in the large numbers that are required for a high throughput screening assay, an approach that would not be possible using primary ADLD patient fibroblasts.

Quantifying lamin B1 expression and associated nuclear abnormalities by HCA.

The human eye can detect lamin B1 overexpression-mediated nuclear abnormalities but the phenotype is subtle, heterogeneous and not observed in all cells. We therefore developed single cell, multiplexed high-content analysis (HCA) to define and quantify lamin B1 overexpression and associated nuclear morphology changes. TRE-LMNB1 MEFs were treated with DOX for 5 days and stained with anti-lamin B1-FITC and anti-lamin A/C-Cy3 primary/secondary antibody pairs. Negative controls included DOX-treated WT and non-induced TRE-LMNB1 cells. Nuclei were counterstained with Hoechst 33342. We decided to use an anti-LMNB1 antibody and not an anti-FLAG antibody because it detects both endogenously and exogenously expressed lamin B1, and reducing either one could lead to a rescue of the nuclear abnormalities. In contrast, a FLAG antibody would only be identifying compounds that reduce the artificially overexpressed FLAG tagged human protein. These might not work on LMNB1 expressed from an endogenous promoter, which is the ultimate objective in patient cells.

Cells were imaged on an Array Scan II high-content reader and analyzed using the Target Activation Bioapplication for lamin B1 and lamin A/C expression, as well as changes in nuclear morphology and texture. Figure 2 shows that differences in WT and TRE-LMNB1 MEFs were quantifiable by HCA. Lamin B1 overexpression was 2–3 fold, mirroring that seen in ADLD patients [6]. DOX response was specific to lamin B1 because lamin A/C levels

and DNA content as measured by Hoechst staining remained unchanged. The assay also quantified lamin B1 nuclear abnormalities as changes in nucleus size, shape, and lamin B1 texture (Figure 2; see Supplemental Table 1 for a detailed description of measured parameters). The negative controls (WT + DOX and unstimulated TRE-LMNB1) showed no significant differences in lamin B1 or nuclear morphology, although Dox in WT cells appeared to cause slight changes in nuclear size (Figure 2). Thus HCA quantified both lamin B1 expression and associated nuclear morphology changes. The response seen with some parameters (lamin B1 levels, S/B = 2.7 ; 5.8%CV; lamin B1 texture, S/B = 2.2, 4.4%CV) indicated that individual lamin B1 response parameters were moderately elevated but tightly distributed, suggesting that the assay could conceivably be developed to HTS robustness, but that further improvements were necessary.

Cell density dependence.

Because cell morphology is dependent on environmental conditions and context, we first performed a cell density dependence study. WT and TRE-LMNB1 MEF were plated at different seeding densities, stimulated for 3 days with DOX, and stained with anti-lamin B1-Cy3 and anti-lamin A/C-Cy5 primary/secondary antibody pairs. Figure 3 shows that lamin B1 expression and associated nuclear abnormalities were highly dependent on cell density, although the separation of stimulated and unstimulated samples was qualitatively maintained across densities. In particular, cell size and length-to-width ratio decreased substantially as cells reached confluency, most likely through crowding effects. Because signal-to-background ratios of the most relevant parameters (lamin B1 intensity and texture, and nuclear shape) between WT and TRE-LMNB1 MEFs were small by HTS standards and further decreased with increasing cell density, maintaining a good separation between positive and negative controls requires a substantial tightening of the data populations at the higher densities. This could be a problem for HTS given the overall heterogeneous phenotype caused by lamin B1 overexpression and the fact the assay is based on primary cells, which could vary substantially from batch to batch. Because the influence of cell density was of similar magnitude to or even exceeded that of the primary parameters measured, this data indicated that cell seeding density would have to be tightly controlled.

Assay optimization.

We next performed a formal HTS assay implementation and validation according to universally accepted guidelines [27]. We first investigated the minimum amount of time needed for lamin B1 levels to return to background after DOX withdrawal in order to recapitulate conditions to be encountered during compound screening. Because there are currently no small molecules that selectively reduce lamin B1, we established reversal of lamin B1 overexpression after DOX withdrawal as a positive control. TRE-LMNB1 MEFs at passage 1 were stimulated for three days with DOX (2 μg/ml) and plated in 384 well plates in the presence or absence of DOX. Cells were fixed and stained every day thereafter with anti-lamin B1 and anti-lamin A/C antibodies and analyzed for lamin B1/AC expression by high content analysis. Supplemental Figure 2 shows that in the presence of DOX, lamin B1 overexpression was maintained for at least four days (left panel, red symbols). After DOX withdrawal, lamin B1 expression returned to near basal levels after two days (left panel, green symbols), which indicates that for screening a two-day exposure to compounds would

be necessary and sufficient to measure a significant reduction in lamin B1. In contrast, DOX withdrawal did not affect lamin A/C or DNA staining intensity (Supplemental Figure 2, middle and right panels).

Improving assay robustness and performance through multivariate analysis.

Nuclear abnormalities caused by lamin B1 expression present as a highly heterogeneous phenotype, with varying expression levels and shape changes across cell populations. The phenotype of lamin B1-induced nuclear abnormalities is a composite of many different features including lamin B1 expression, but also the appearance of indentations, invaginations, or contortions, and excessive surface folding (Figure 1D). A human observer processes these observations based on experience and context, and thus can classify objects as “normal” or “abnormal” (Figure 1E). For screening this is obviously not feasible. On the other hand, when measured quantitatively, the primary parameter of interest, lamin B1 expression, on occasion yielded HTS performance (i.e., Z-factors > 0.5) but this was not observed consistently. To more robustly quantify the cellular phenotype of lamin B1 expression and associated nuclear morphologies, we developed multivariate analysis methodology (Linear Discriminant Analysis, LDA [28], similar to what we previously developed for zebrafish [19] and yeast [20]). Figure 4 illustrates the extent to which LDA improved the analysis. Lamin B1-mediated nuclear abnormalities can be seen with the naked eye but are present in both positive (TRE-LMNB1) and negative (WT) samples, do not present uniformly across the image, and occur only in a subset of cells. “Histo-box” plots that we developed for heterogeneity analysis of cell populations [18] expose quantitative differences in the distribution of several cell features (Figure 4B), suggesting that the analysis would benefit from Heterogeneity Indices that we recently developed to capture biologically relevant heterogeneity in cell populations [18].

The final parameter set encompassed nine intensity and texture measurements (mean, total, and variance of lamin B1, lamin A/C, and Hoechst), three shape measurements (area, circularity, elongation), 12 cell-to-cell intensity distribution parameters (prefix SD_) and three heterogeneity measurements (KS_norm, denoting deviation from normal distribution, % outliers, and quadratic entropy (QE), denoting differences in the shape of data distributions [18])(Figure 4C and Supplemental Table 1). LDA dramatically improved separation between minimum and maximum signals compared with each individual parameter alone (illustrated in Figure 4C for lamin B1 expression; a full set of data and descriptions of the HCA parameters can be found in Supplemental Table 1), to a point where the method separated positive and negative controls with a Z-factor of 0.89 (Figure 4C). Furthermore, LDA weighted features that distinguished the two classes (Supplemental Table 1, *LDA Loading*), thus not only improving assay performance but defining the phenotype of nuclear abnormalities. The results document that LDA quantitatively captured lamin B1-mediated nuclear abnormalities, and rendered the assay suitable for HTS implementation.

Final HTS implementation.

Based on the results from the optimization studies, the assay was subjected to a formal three-day variability assessment consisting of two full microplates of positive (+ DOX) and negative controls (two days of DOX withdrawal to mimic compound treatment) on three

different days. The assay met accepted HTS standards on all three days with the same level of statistical significance, documenting screening readiness (Supplemental Figure 3). We also devised a strategy to deal with batch-to-batch variability, which is based on analysis of "sentinel" cells the week before a large-scale run is performed (Figure 5). This design ensures that the particular batch of primary cells to be used in HTS responds to DOX with lamin B1 expression in a manner to anticipate screenability. The strategy reduces the risk losing an entire experimental run due to failure of cells to respond to DOX.

DISCUSSION

We have developed an HTS ready cellular assay to detect lamin B1 overexpression and associated nuclear abnormalities. Lamin B1 overexpression is the genetic cause for ADLD, a debilitating demyelinating disease for which no treatments exist. While the precise mechanisms linking the genetic defect to demyelination and the biological consequences of nuclear abnormalities are not known, changes in nuclear architecture are a direct result of lamin B1 overexpression because they revert to normal when lamin B1 levels are reduced, either by siRNA or, in our model, by withdrawing the overexpression stimulus. ADLD is a late onset disease, which presents a large window of opportunity for therapeutic intervention. We posit that small molecules that reduce lamin B1 levels and revert associated nuclear abnormalities could prevent disease onset and/or progression.

There are some obstacles in the development of an assay measuring a reduction in lamin B1 levels. First, the extent of lamin B1 overexpression in ADLD patient fibroblasts is very small when measured on a well average level (Supplemental Figure 1). Second, the relevant cell type responsible for the demyelinating defect are oligodendrocytes, which are not available for screening. Third, the phenotype of lamin B1-mediated nuclear abnormalities in patient derived cells is extremely heterogeneous and only seen in a small percentage of cells. We therefore developed a mouse model of DOX-inducible lamin B1 overexpression (TRE-LMNB1), which allows for generation of an unlimited number of cells for screening. Fibroblasts from TRE-LMNB1 mice overexpress pathophysiologically relevant levels of lamin B1 and show nuclear abnormalities seen in ADLD patients. Importantly, the phenotype reverses after DOX withdrawal; both lamin B1 overexpression and nuclear abnormalities return to levels seen in normal cells. Therefore, the mouse model has good face and construct validity. However, we recognize that an inherent weakness of our cell culture model is that it does not include the endogenous LMNB1 promoter driving the overexpression. Compounds that we identify will be only those that can reduce LMNB1 at the protein level and will not include molecules that reduce LMNB1 expression levels through transcriptional inhibition.

The phenotype of lamin B1 mediated nuclear abnormalities can be visualized by immunocytochemistry and quantified by a human observer. This is an extemely laborious process that limits utility of the method to small numbers of samples. We used high content screening to automatically acquire images and perform preliminary measurements on lamin B1 and nuclear morphology. Initial experiments showed a 2–3 fold increase in lamin B1 (Figure 2) confirming the results of Western blots (Figure 1). DOX stimulation did not change levels of lamin A/C or DNA content, documenting specificity of the system.

Changes in nuclear morphology were highly dependent on cell density. This was not surprising as the environment in which cells are grown is known to determine cell size and shape. However we found that not all parameters were equally affected. Regardless of stimulation, cells at higher densities assumed a more rounded shape, became more compact and regularly shaped, showed decreased levels of lamin B1 and lamin A/C as measured by immunocytochemistry, but increased DNA staining. DOX stimulation caused a substantial difference in lamin B1 associated measurements and nuclear morphology that remained measurable for some parameters (lamin B1 intensity and texture, nucleus elongation and shape irregularity). Differences in nucleus size became apparent only at high density, whereas differences in lamin A/C levels and texture (if any), remained constant. Importantly, the magnitude of changes due to cell density was comparable to that caused by lamin B1 overexpression, thereby obscuring, counteracting, canceling, or even outweighing changes caused by lamin B1 expression. Furthermore, at a high initial cell seeding density DOX was unable to sustain ectopic lamin B1 expression on day three and four (data not shown), likely because of cells attaining quiescence due to contact inhibition. This indicated that too high a seeding density might be unsuitable for screening because of a collapse in assay window. On the other hand, very low densities present a challenge for HTS as the time required to collect meaningful numbers of cells could substantially limit throughput. Therefore cell density had to be carefully optimized and tightly controlled.

In order to overcome heterogeneity, we developed a multiparametric analysis that attempts to fully capture the heterogeneous nature of lamin expression, nuclear morphoplogy, and distribution across cell populations. To quantify the phenotype as a human observer would, we developed a numerical measure to classify nuclei and “normal” and “abnormal”. Our method of choice was LDA, which separates cell populations into two classes through linear combination of multiple features. Because LDA extracts maximum information from fluorescence images, it has the potential to dramatically improve separation of classes compared with individual features alone.

We measured twenty-seven individual parameters derived from cell segmentation. No single parameter reliably and repeatedly yielded HTS performance, but some parameters came close in some experiments and described the phenotype better than others. In the sample data set summarized in Supplemental Table 1, The best differentiating parameter was QE, which measures differences in the shape of data distributions [18]. This parameter therefore quantified the visually apparent increase in cellular heterogeneity upon DOX stimulation. Lamin B1 levels and texture were the parameters that best differentiated cells based on direct lamin B1 measurements. Those parameters also contributed substantially to LDA weighting (note that absolute numbers indicate the degree to which the parameter contributes to the classifier, with larger values denoting larger contributions), indicating that LDA captured the most important biological events. Other parameters showed decent Z-factors but lacked informativeness as their S/B were small (P2A and LWR, 5% increase). Others had large S/B but small Z-factors suggesting high variability (e.g., cell-to-cell distribution of lamin B1 texture). Importantly, LDA weighting and the extent of separation of stimulated and unstimulated cell populations for individual parameters changed from experiment to experiment. LDA consolidated the collective changes into a single “lamin B1-mediated nuclear abnormalites” parameter, much like a human observer would, and rendered the assay

reliable and robust enough to satisfy HTS criteria in multi-day variability assessments (Supplemental Figure 3). We should note that the ultimate proof of utility will be how well the method performs under conditions used in screening, and pilot library screening is currently underway. Because the three-day variability assessments represent an extremely rigorous analysis, we expect the assay will be a suitable plate QC criterion separating positive and negative controls during screening, when numbers of control wells are much smaller.

ADLD is a devastating and debilitating disease for which no treatments exist. It is a monogenic disease caused by lamin B1 gene duplication and protein overexpression, suggesting that reducing lamin B1 levels could be a viable therapeutic strategy. To discover small molecules that reduce lamin B1 expression we created a cell culture model that recapitulates the underlying cause of the disease, and developed a robust HCS assay that meets stringent HTS requirements. It is our hope that this assay, when executed in HTS, will identify compounds that reduce lamin B1 levels and associated nuclear abnormalities. We posit that such agents could be valuable starting points for the development of ADLD therapeutics.

Supplementary Material

Refer to Web version on PubMed Central for supplementary material.

ACKNOWLEDGEMENTS

We thank Harold Takyi for technical assistance. This work was supported by NIH grants R33NS106087 to AV/QSP and R01NS095884, R21NS104384 to QSP.

Abbreviations:

ADLD	Autosomal Dominant Leukodystrophy
BSA	bovine serum albumin
Cy3	indocarbocyanine with three-carbon linker
Cy5	indocarbocyanine with five-carbon linker
DMSO	dimethyl sulfoxide
DOX	doxycycline
HCA	high-content analysis
FITC	fluorescein isothiocyanate
HTS	high-throughput screening
LDA	linear discriminant analysis
LWR	length-to-width ratio
MEF	mouse embryonic fibroblast

P2A	perimeter-to-area ratio
PCR	polymerase chain reaction
WT	wild type
TRE	tetracycline responsive element

REFERENCES

1. Padiath QS; Fu YH Autosomal dominant leukodystrophy caused by lamin B1 duplications a clinical and molecular case study of altered nuclear function and disease. Methods Cell Biol 2010, 98, 337–57. [PubMed: 20816241]
2. Finnsson J; Sundblom J; Dahl N; et al. LMNB1-related autosomal-dominant leukodystrophy: Clinical and radiological course. Ann Neurol 2015, 78, 412–25. [PubMed: 26053668]
3. Padiath QS; Saigoh K; Schiffmann R; et al. Lamin B1 duplications cause autosomal dominant leukodystrophy. Nat Genet 2006, 38, 1114–23. [PubMed: 16951681]
4. Nmezi B; Giorgio E; Raininko R; et al. Genomic deletions upstream of lamin B1 lead to atypical autosomal dominant leukodystrophy. Neurol Genet 2019, 5, e305. [PubMed: 30842973]
5. Giorgio E; Robyr D; Spielmann M; et al. A large genomic deletion leads to enhancer adoption by the lamin B1 gene: a second path to autosomal dominant adult-onset demyelinating leukodystrophy (ADLD). Hum Mol Genet 2015, 24, 3143–54. [PubMed: 25701871]
6. Giorgio E; Rolyan H; Kropp L; et al. Analysis of LMNB1 duplications in autosomal dominant leukodystrophy provides insights into duplication mechanisms and allele-specific expression. Hum Mutat 2013, 34, 1160–71. [PubMed: 23649844]
7. Butin-Israeli V; Adam SA; Goldman AE; et al. Nuclear lamin functions and disease. Trends Genet 2012, 28, 464–71. [PubMed: 22795640]
8. Gruenbaum Y; Foisner R Lamins: nuclear intermediate filament proteins with fundamental functions in nuclear mechanics and genome regulation. Annu Rev Biochem 2015, 84, 131–64. [PubMed: 25747401]
9. Stewart CL; Roux KJ; Burke B Blurring the boundary: the nuclear envelope extends its reach. Science 2007, 318, 1408–12. [PubMed: 18048680]
10. Gerace L; Huber MD Nuclear lamina at the crossroads of the cytoplasm and nucleus. Journal of structural biology 2012, 177, 24–31. [PubMed: 22126840]
11. Jung HJ; Lee JM; Yang SH; et al. Nuclear lamins in the brain - new insights into function and regulation. Molecular neurobiology 2013, 47, 290–301. [PubMed: 23065386]
12. Ferrera D; Canale C; Marotta R; et al. Lamin B1 overexpression increases nuclear rigidity in autosomal dominant leukodystrophy fibroblasts. FASEB J 2014, 28, 3906–18. [PubMed: 24858279]
13. Barascu A; Le Chalony C; Pennarun G; et al. Oxidative stress induces an ATM-independent senescence pathway through p38 MAPK-mediated lamin B1 accumulation. EMBO J 2012, 31, 1080–94. [PubMed: 22246186]
14. Heng MY; Lin ST; Verret L; et al. Lamin B1 mediates cell-autonomous neuropathology in a leukodystrophy mouse model. J Clin Invest 2013, 123, 2719–29. [PubMed: 23676464]
15. Rolyan H; Tyurina YY; Hernandez M; et al. Defects of Lipid Synthesis Are Linked to the Age-Dependent Demyelination Caused by Lamin B1 Overexpression. J Neurosci 2015, 35, 12002–17. [PubMed: 26311780]
16. Jozefczuk J; Drews K; Adjaye J Preparation of mouse embryonic fibroblast cells suitable for culturing human embryonic and induced pluripotent stem cells. J Vis Exp 2012.
17. Agresti A; Coull BA Approximate is better than “exact” for interval estimation of binomial proportions. Am Stat 1998, 52, 119–126.
18. Gough AH; Chen N; Shun TY; et al. Identifying and quantifying heterogeneity in high content analysis: application of heterogeneity indices to drug discovery. PLoS One 2014, 9, e102678. [PubMed: 25036749]

19. Shun T; Gough AH; Sanker S; et al. Exploiting Analysis of Heterogeneity to Increase the Information Content Extracted from Fluorescence Micrographs of Transgenic Zebrafish Embryos. Assay Drug Dev Technol 2017, 15, 257–266. [PubMed: 28800244]

20. Ngo M; Wechter N; Tsai E; et al. A High-Throughput Assay for DNA Replication Inhibitors Based upon Multivariate Analysis of Yeast Growth Kinetics. SLAS Discov 2019, 24, 669–681. [PubMed: 30802412]

21. Dürr O; Duval F; Nichols A; et al. Robust hit identification by quality assurance and multivariate data analysis of a high-content, cell-based assay. J Biomol Screen 2007, 12, 1042–9. [PubMed: 18087069]

22. Kümmel A; Gubler H; Gehin P; et al. Integration of multiple readouts into the z' factor for assay quality assessment. J Biomol Screen 2010, 15, 95–101. [PubMed: 19940084]

23. Zhang JH; Chung TDY; Oldenburg KR A simple statistical parameter for use in evaluation and validation of high throughput screening assays. Journal of Biomolecular Screening 1999, 4, 67–73. [PubMed: 10838414]

24. Nmezi B; Xu J; Fu R; et al. Concentric organization of A- and B-type lamins predicts their distinct roles in the spatial organization and stability of the nuclear lamina. Proc Natl Acad Sci U S A 2019, 116, 4307–4315. [PubMed: 30765529]

25. Backman CM; Zhang Y; Hoffer BJ; et al. Tetracycline-inducible expression systems for the generation of transgenic animals: a comparison of various inducible systems carried in a single vector. J Neurosci Methods 2004, 139, 257–62. [PubMed: 15488239]

26. Ryding AD; Sharp MG; Mullins JJ Conditional transgenic technologies. J Endocrinol 2001, 171, 1–14. [PubMed: 11572785]

27. Iversen PW; Beck B; Chen YF; et al. HTS Assay Validation In Assay Guidance Manual; Sittampalam GS; Coussens NP; Brimacombe K; et al., Eds.; Eli Lilly & Company and the National Center for Advancing Translational Sciences: Bethesda (MD), 2004.

28. McLachlan GJ Discriminant Analysis and Statistical Pattern Recognition. Wiley Interscience: Hoboken, N.J, 2004.

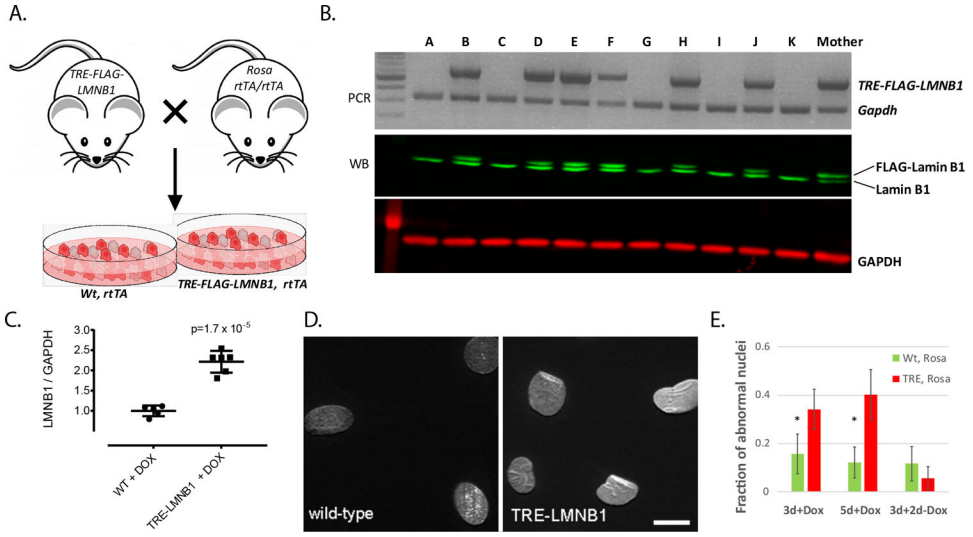

Figure 1. Generation of a mouse model of inducible lamin B1 expression.

A. Mating strategy to generate TRE-FLAG-LMNB1;Rosa rtTA embryonic fibroblasts. MEFs were isolated from embryos at E13.5, genotyped, and lamin B1 expression verified by Western blot. **B.** Western blot of MEFs treated with doxycycline (DOX) to overexpress exogenous FLAG-LMNB1. The presence of FLAG causes exogenous lamin B1 to migrate slightly slower than endogenous lamin B1, resulting in a double-band. **C.** Quantification of Western blots in B. **D.** Immunofluorescence staining of MEF nuclei with an anti-lamin B1 antibody reveals abnormal folds and wrinkles in the nuclear envelope owing to overexpression of lamin B1. **E.** Nuclear abnormalities were reversible upon DOX removal. Y-axis shows percentage of abnormal nuclei as quantified by visual examination and manual classification as described in Materials and Methods. Error bars – 95% confidence intervals, *-p<0.05.

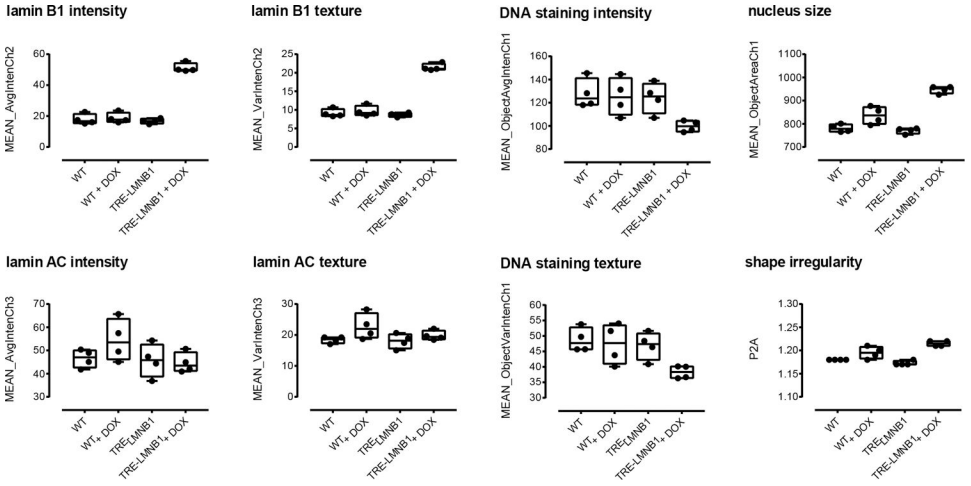

Figure 2. Initial quantification of lamin B1 expression and nuclear morphology by high-content analysis.

WT and TRE-LMNB1 MEF were cultured in 96 well plates for three days in the presence or absence of DOX and immunostained with anti-lamin B1/lamin A/C antibodies. Plates were scanned on an ArrayScan II HCS reader and analyzed for lamin expression and nuclear texture by the Target Activation Bioapplication as described in Materials and Methods. Each box plot shows the mean, first and third quartiles, and range of four wells from a single experiment that has been repeated at least three times.

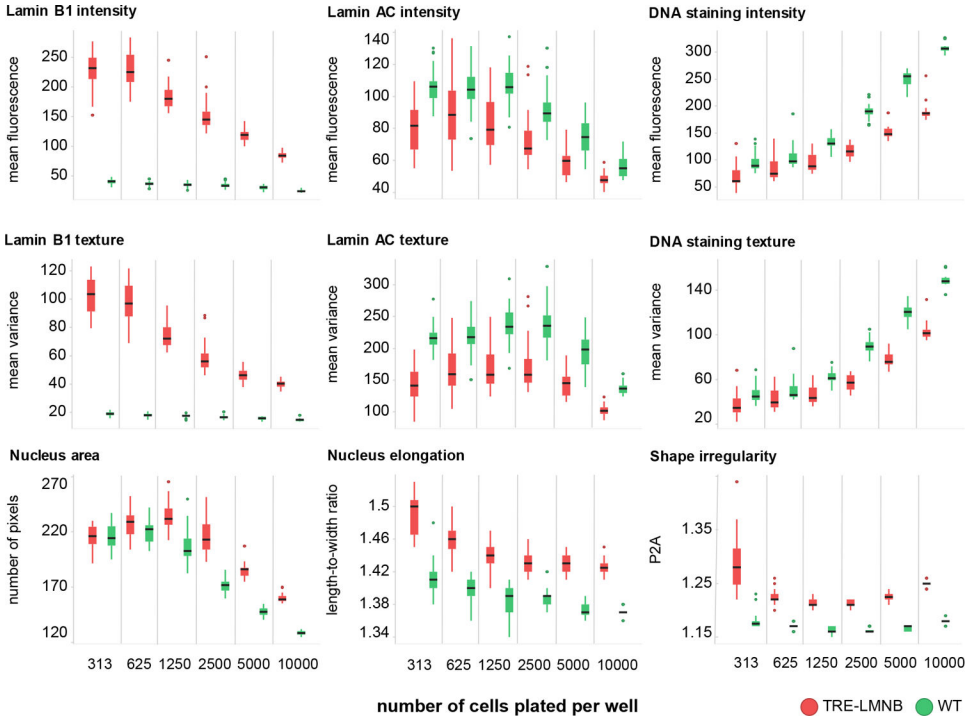

Figure 3. Effects of lamin B1 overexpresson are dependent on cell density.

WT or TRE-LMNB1 MEF were seeded at different densities and analyzed by HCA three days after DOX stimulation. Most parameters were strongly affected by cell density, however for some differences between WT and lamin B1 overexpressing MEFs were retained. Each box plot shows the mean, first and third quartiles, and range of 7–14 technical replicates from a single experiment that has been repeated twice. Green, WT ; red, TRE-LMNB1 MEF.

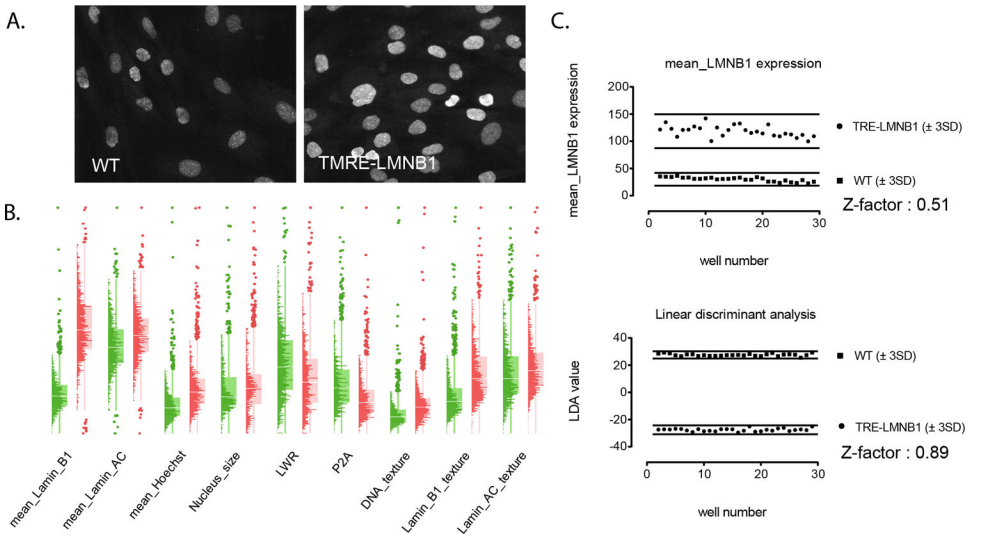

Figure. 4. Exploiting multiple features to fully capture complexity and heterogeneity of lamin B1 overexpression and associated nuclear abnormalities.

Images in **A.** show two randomly chosen fields of Lamin B1 stained nuclei from wild-type and transgenic MEFs that illustrate the heterogeneity of nuclear abnormalities. Images were taken with a 40X objective on an ImageXpress Ultra confocal HCS reader. **B.** Histo-Box plots expose dissimilarities in the distribution of cell and well features not easily appreciated by visual inspection. Green graphs are WT, and red graphs are TRE-LMNB1. Each plot is the aggregate of individual cells from 30 wells, with each well containing a minimum of 1,000 cells. Note that only a subset of parameters is shown for clarity; the full set of parameters can be found in Supplemental Table 1. **C.** Linear discriminant analysis of 24 cell and well features and three heterogeneity indices was used to integrate information from multiple features into a single readout that provided maximum separation between the two datasets, resulting in a dramatic improvement in assay performance compared with lamin B1 expression alone. Note that LDA returns identical absolute values for the two classes, therefore an S/B cannot be established.

A. **Sentinel cell procedure to assess batch-to-batch responsiveness and assay performance**

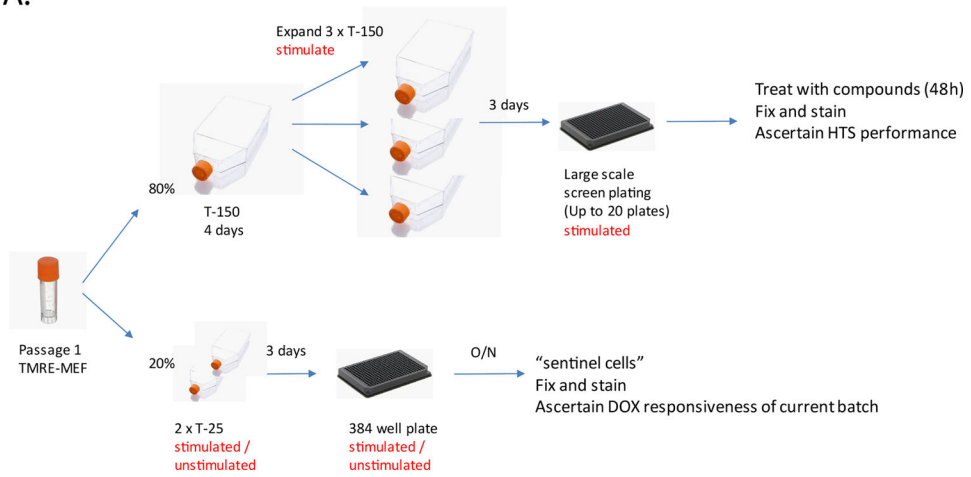

B. **Batch-to-batch variability**

	trial 1			trial 2			trial 3			trial 4		
	S/B	%CV	Z-prime	S/B	%CV	Z-prime	S/B	%CV	Z-prime	S/B	%CV	Z-prime
LMNB1 levels	2.7	17	0.41	2.5	7	0.65	2.4	5	0.37	3.9	13	0.51
LMNB1 texture	2.2	15	0.4	1.7	5	0.49	2.4	5	0.04	2.9	8	0.49

Figure 5. Sentinel cell design to ascertain batch-to-batch responsiveness, assay performance and to eliminate risk of failure during HTS.

A. HTS workflow. From a single vial of primary cells, a small portion is set aside after thawing and left unstimulated or stimulated for 3 days with DOX to induce expression of lamin B1. The majority of cells is expanded into multiple flasks and stimulated for experiments after the second split. Because the sentinel cells are from the same vial and are processed before the large batch gets exposed to compounds, unresponsive batches are identified before a large scale screen is executed, eliminating the risk of losing precious library compounds during HTS. **B. Assessment of batch-to-batch variability.** Table shows canonical HTS measures obtained on different days with different batches of TRE-MEF. Data for each experiments are based on four technical replicates.